

QC
851
.T45
no. 51

SURFACE WINDS AND OIL SLICK TRANSPORT CALCULATED FROM
ROSSBY NUMBER SIMILARITY THEORY

Fredricksen and Wagner

Report No. 51

June 1979

ATMOSPHERIC
SCIENCE GROUP



The University of Texas
College of Engineering
Austin, Texas 78712

QC
851
.T45
no. 51

ATMOSPHERIC SCIENCE GROUP
College of Engineering
The University of Texas
Austin, Texas

ABSTRACT

Rossby number similarity theory has been used to calculate surface winds and transport of an oil slick over the ocean. Calculations were

Report No. 51

June 1979

for the month of December, 1978. When buoyancy was included, agreement of calculations with observed data was very good. The model has been

¹¹ SURFACE WINDS AND OIL SLICK TRANSPORT
CALCULATED FROM ROSSBY NUMBER SIMILARITY THEORY

was significant that either of the other two parameters is predicted as well as the observed data.

SILVER SPRING
CENTER

'JUL 2 1979

N.O.A.A.
U. S. Dept. of Commerce

by
Ellin J. Fredricksen
and

Norman K. Wagner

Prepared for the
Techniques Development Laboratory
National Weather Service
National Oceanic and Atmospheric Administration
U.S. Department of Commerce
under Contract MO-A01-78-00-4118

ABSTRACT

Rossby number similarity theory has been used to calculate surface winds and transport of an oil slick over the ocean. Calculations were compared with observed data from the ARGO MERCHANT wreck site during the month of December, 1976. When baroclinicity was included, agreement of calculations with observed data was very good. The model has been run with different limitations on the roughness parameter, the drag coefficient, and the baroclinicity. Baroclinicity appeared to be much more significant than either of the other two parameters in producing an oil slick path resembling the observed slick.

TABLE OF CONTENTS

Chapter	Page
I. INTRODUCTION	1
II. ROSSBY NUMBER SIMILARITY THEORY	3
III. THE MODEL	7
No-Slip Model	9
Barotropic Conditions	9
Baroclinic Conditions	10
Sensitivity Analysis of No-Slip Model	12
Stability effects	12
Baroclinic effects	14
Drift Model	18
Changes in Code to Accomodate Surface Drift	18
Verification	21
IV. OIL TRANSPORT	22
Prediction of Winds	22
Transport of Oil	27
Discussion	29
V. CONCLUSION	33
APPENDICES	35
REFERENCES	44

LIST OF FIGURES

Figure		Page
1.	The non-dimensionalized ten-meter wind as a function of stability in a barotropic boundary layer	13
2.	The geostrophic drag coefficient behavior under diabatic conditions	15
3.	Universal functions A and B as a function of stability	17
4.	The change in the cross-isobaric angle due to baroclinicity	19
5.	Location of the ARGO MERCHANT oil plume on 27 December 1976 compared with the plume centerlines calculated from observed winds and from model winds for Cases 1a and 1b	30

CHAPTER I

INTRODUCTION

ARGO MERCHANT. AMOCO CADIZ. BRAVO. Oil gushes forth onto the sea, destroying wild life in its path and wild, scenic beauty on the coasts of three continents. Can we determine where this oil will go? Will it touch land? The answers depend upon our ability to predict the transport of oil on the ocean. This research evolved a model to aid in the study of oil slick movement and winds near the earth's surface.

The model was derived by employing Rossby number similarity theory and was implemented on the CDC 6600 Computer in FORTRAN. Rossby number similarity describes the planetary boundary layer (PBL) by the surface Rossby number, the geostrophic drag coefficient, the von Karman constant k , and two universal functions. The surface Rossby number is defined as the non-dimensional product of the magnitude of the mean surface geostrophic wind V_g , the Coriolis parameter f , and the surface roughness height z_0 such that $R_0 = V_g / fz_0$. The geostrophic drag coefficient is another non-dimensional product, defined as $c_g = u_* / V_g$, where u_* is the friction velocity. The universal functions have been empirically determined for neutral, diabatic, and baroclinic cases (e.g., Clarke & Hess, 1974, 1975; Arya & Wyngaard, 1975), and it was these functions which were incorporated into the model. The input to the model was easily obtainable meteorological

data (vertical and horizontal temperature gradients, sea-level atmospheric pressure data). Using this data, the model produced a reasonable estimate of surface winds, sea surface drift, and movement of an oil slick.

The first model which was studied employed a no-slip lower boundary to coincide with the conditions under which the universal functions were derived. The neutral, barotropic model was then expanded to accommodate the most general diabatic, baroclinic cases. Sensitivity studies were run and results were compared with observed data of Clarke & Hess (1974, 1975) and Hasse & Dunckel (1974). The reasonable agreement with observed data suggested this portion of the model was working properly.

The next addition to the model was the incorporation of sea surface drift. The drift model was derived by coupling a moving lower boundary to the atmosphere. To do this, the surface drift was assumed to be equal in magnitude to the friction velocity and to be in the direction of the surface geostrophic wind. The drift velocities produced by this model were used to forecast the advection of hypothetical "oil slicks" downstream. The mass of these slicks was assumed constant and only the mean motion of the slick centroids was considered. Oil slick motion and wind speed and direction obtained from the model were compared to data collected during the investigation of the ARGO MERCHANT oil spill of December 15, 1976. Although this spill occurred within 30 nautical miles of land, where mesoscale effects and currents (not included in the model) could be important, the model results compared favorably with the observations. Thus, Rossby number similarity theory appears to be applicable to the problem of determining surface winds and oil slick movement over the open ocean.

CHAPTER II

ROSSBY NUMBER SIMILARITY THEORY

Outside of the ivory towers and laboratory, it is difficult to undertake controlled experiments to understand and measure nature. We are fortunate to have another tool at our disposal--similarity theory. Using this theory, we attempt to select the variables governing the phenomenon in question, non-dimensionalize them with scaling variables, and organize them such that they might yield universal functions.

Consider the flow within the neutral, steady state barotropic planetary boundary layer (PBL). This flow is essentially governed by a height z within the layer, the geostrophic wind speed V_g , the Coriolis parameter f , and the surface roughness length z_0 . One can presume that this flow is a function of the non-dimensional ratio V_g/fz_0 , known as the surface Rossby number R_0 . The equations of motion for this flow, with horizontally homogeneous turbulence, and without heat transfer are

$$(A) \quad -f(\bar{v} - \bar{v}_g) = -\frac{d}{dz} (\overline{u'w'}) \quad (1)$$

and

$$f(\bar{u} - \bar{u}_g) = -\frac{d}{dz} (\overline{v'w'}), \quad (2)$$

where \bar{u} , \bar{v} , and \bar{u}_g , \bar{v}_g are the horizontal x- and y-components of the mean boundary layer and geostrophic winds, and u' , v' , and w' are the horizontal and vertical velocity fluctuations. We wish to non-dimen-

sionalize these equations for the boundary layer and keep them well-behaved at both some scale height h above the surface and at z_0 near the earth's surface. Hence we want to select an appropriate scaling velocity to make the scaled flow field independent of z_0/h , and thus finite.

Orienting the flow field such that the x-axis is aligned with the surface stress, we begin to non-dimensionalize the equations with the surface stress $\tau_x = \rho u_*^2$, $\tau_y = 0$. Then,

$$-\frac{f}{\rho} \frac{(\bar{v} - \bar{v}_g)}{u_*} = \frac{-d(\overline{u'w'})}{dz} / \rho u_*^2$$

and likewise for equation (2). Furthermore,

$$\frac{(\bar{v} - \bar{v}_g)}{u_*} = \frac{\rho}{f/u_*} \frac{d(\overline{u'w'})}{dz} / \rho u_*^2$$

so that we have a non-dimensional set of equations, not explicitly dependent upon V_g/fz_0 (the governing variables in non-dimensional form), with a scale velocity u_* (the friction velocity) and scale height $h = u_*/f$:

$$\frac{\bar{v} - \bar{v}_g}{u_*} = \frac{d(\overline{u'w'})/u_*^2}{d z f/u_*} \quad (3)$$

$$\frac{\bar{u} - \bar{u}_g}{u_*} = \frac{-d(\overline{v'w'})/u_*^2}{d z f/u_*} \quad (4)$$

However, since V_g/u_* is implicitly a function of V_g/fz_0 , we approach a stress singularity near the surface in the formal limit process as $V_g/fz_0 \rightarrow \infty$. Thus we can assume the above equations to be valid in an outer layer and must reevaluate the scaling factors for flow near the lower boundary, the inner or surface layer.

Near the surface, z/z_0 is finite and thus useful for a non-dimensional height, and in the formal limit as $v_g/fz_0 \rightarrow \infty$, the flow cannot "feel" the geostrophic wind, so we are left with

$$\frac{\bar{v}}{u_*} = f_y \left(\frac{z}{z_0} \right) \quad (5)$$

and

$$\frac{\bar{u}}{u_*} = f_x \left(\frac{z}{z_0} \right) \quad (6)$$

The next step is to solve these equations and determine the final non-dimensional description of the flow field within the PBL, with the restrictions of neutral stratification and no heat transfer, as mentioned above. This can be accomplished by matching the inner and outer layers, requiring the similarity laws for the inner and outer layers to be the same in the limit as both $zf/u_* \rightarrow 0$ and $z/z_0 \rightarrow \infty$ simultaneously. This is accomplished by matching the x-component of wind shear $\frac{\partial \bar{u}}{\partial z}$ for both (4) and (6) and doing likewise for $\frac{\partial \bar{v}}{\partial z}$ with equation (3) and (5). For a complete discussion of this process see Blackadar and Tennekes (1968). The resulting equations, after separation of variables and integration, satisfying the boundary conditions, are

$$\frac{\bar{u}}{u_*} = \frac{1}{k} \ln \frac{z}{z_0} \quad (7)$$

and

$$\frac{\bar{u}_g}{u_*} = \frac{1}{k} \left[\ln \frac{u_*}{fz_0} - A \right] \quad (8)$$

when matching x-components, and similarly for y-components,

$$\frac{\bar{v}_g}{u_*} = \frac{-B}{k} \quad (9)$$

where A and B are universal functions, constants when the atmosphere is neutral and barotropic. Using equations (8) and (9), simple algebra takes

us to the equations of Rossby number similarity:

$$\ln(R_o) = A - \ln \frac{u_*}{v} + \left(\frac{k^2 V_g^2}{u_*^2} - B^2 \right)^{1/2} \quad (10)$$

$$\sin \alpha = \frac{B}{k} \frac{u_*}{V_g} \quad (11)$$

where α is the cross-isobaric angle and u_*/V_g is the geostrophic drag coefficient c_g .

CHAPTER III

THE MODEL

Similarity theory requires that the non-dimensional functions involved be determined experimentally. This has been done with Rossby number similarity theory by Clarke & Hess (1975) and Arya (1975). If these constants have been determined correctly, we should be able to apply the theory, using these functions, at any location. Hence a computer model was developed to apply this theory to the problem of calculating surface winds in the boundary layer and surface drift of the ocean's waters.

The computer model was run in FORTRAN on the CDC 6600/6400 computer of the University of Texas at Austin. The code consisted of a driver and two subroutines, WIND and GWIND (see Appendix A). GWIND calculated geostrophic wind and direction and oriented the axes to determine thermal wind components. WIND utilized Rossby number similarity theory to calculate the cross-isobaric angle α , the friction velocity u_* , the surface roughness length z_0 , and the 10 meter surface wind U (or U_{10}). Since the equations are non-linear, an iterative technique was employed to determine u_* and z_0 . The non-dimensional functions, functions of stability μ and baroclinicity S , were redefined to allow for these conditions. Later a moving lower boundary was added to simulate water below the atmosphere.

Given the horizontal temperature gradient, air-sea temperature difference, mean air column temperature, and the surface geostrophic wind

speed and direction, the model determined the friction velocity u_* and the cross-isobaric angle α . From these, a drag coefficient c_d was used to calculate the surface wind speed and direction.

The universal functions A and B were determined using stability coefficients derived from Arya (1975) and baroclinic coefficients from Clarke & Hess (1975). Using Rossby number similarity, it is possible to define a function $F(c_g) = \ln R_o - A + \ln(c_g) - \left(\frac{k^2}{c_g} - B^2\right)^{1/2}$ (see equation 10) and its derivative $F'(c_g)$. For the barotropic case (see Appendix B), we solve for either neutral or diabatic conditions. For neutral stability, $A = A_o = 1.1$, $B = B_o = 4.3$ (Clarke & Hess, 1974); otherwise the stability parameter μ is calculated, and thereafter A and B are computed as a function of μ , which is defined according to Hasse & Dunckel (1974) such that

$$\mu = \frac{k^2 g (T_a - T_o)}{fUT_a},$$

which differs from the μ of Clarke & Hess, among others, as discussed below. $(T_a - T_o)$ is the air-sea temperature difference, T_a the air temperature (also referred to as T, for notation simplicity), and g the acceleration of gravity.

Knowing $F(c_g)$ and $F'(c_g)$, Newton's Method is utilized to solve for c_g by iteration. Then $u_* = (c_g)(V_g)$. The surface roughness length z_o was updated using Charnock's equation such that $z_o = \mu u_*^2 / g$ where $m = 0.016$ and $g = 981 \text{ cm/sec}^2$. Convergence was assumed when z_o changed by less than a specified small amount.

The surface wind was computed as $U_{10} = u_* / \sqrt{c_d}$ where c_d , the surface drag coefficient, is initially a constant 1.24×10^{-3} . This value was chosen in order to compare results with those of Hasse & Dunckel (1974),

which were taken from observations over the open ocean. It is also a reasonable mean value of the drag coefficients determined by Deacon (1973a), Hsu (1974), Smith & Banke (1975), and others in the literature. Hsu and others have also reminded us that stability can be a factor in determining the drag coefficient. Stability affects u_* , and this in turn affects the value attributed to c_d . However, since in this model, u_* is determined by using A and B as functions of stability, this could allow the constant c_d to be used to calculate U_{10} . The drag coefficient will be modified for results over the open ocean and will be discussed further in the section on the Drift Model. The model was then run to compare output values with those determined by other investigators.

No-Slip Model

Barotropic Conditions

Recall that a neutral, steady state, barotropic PBL was a basic assumption for Rossby number similarity theory. Under these conditions, the universal functions A and B are constants, $A = 1.1$ and $B = 4.3$.

A glance at most thermodynamic diagrams of the lower atmosphere will show that the boundary layer is seldom neutral over a period of time. Thus, stability of the layer must also be considered when determining A and B. The stability parameter can be determined from the Obukhov length $L = \frac{-u_*^3 T_a \rho c_p}{k g Q_h}$, where c_p is the specific heat capacity at constant pressure, ρ is the density of air, T_a is the mean air column temperature and Q_h is the heat flux, assumed to be $Q_h = \rho c_p D U (T_o - T_a)$, and D is the heat transfer coefficient. Given that $\mu = k u_* / f L$, substitution of terms yield

$$\mu = - \frac{k^2 g D U (T_o - T_a)}{f c_d U^2 T_a}$$

recalling that $c_d = (u_*^2/U)^2$. Then, if we assume that D and c_d vary similarly with respect to air-sea temperature differences and that they are of approximately the same magnitude (Hicks, 1974; SethuRamen & Raynor, 1975), they will counteract each other and leave us with

$$\mu \approx \frac{k^2 g (T_a - T_o)}{fUT_a} = \mu',$$

the μ' as defined by Hasse & Dunckel (1974) and written as μ hereafter.

Arya (1975) has determined coefficients for μ to show how A and B vary with stability. However, since μ will not be as large over the ocean as over land, generally $|\mu| \leq 90$, his cubic term can be neglected.

Slightly modifying the other coefficients to compensate for this, we have

$$\begin{aligned} A(\mu) &= A_o - 0.10 \mu - 0.001 \mu^2 \\ B(\mu) &= B_o + 0.13 \mu - 0.001 \mu^2, \end{aligned}$$

where A_o and B_o are the neutral, barotropic values for A and B . The computer model, however, is still sensitive to this stability parameter and will not converge for values $|\mu| \geq 70$ under barotropic conditions. This limitation should still be sufficient for most oceanic applications.

Baroclinic Conditions

Baroclinic conditions in the atmosphere must also be considered in a boundary layer model. Temperature advection and simple differences in insolation heating will contribute to baroclinicity. Hence, the universal functions A and B must be adjusted for baroclinicity S as well as stability μ .

Clarke & Hess (1975), assumed $h = u_*^2/f$ to be the appropriate scale height in the boundary layer, and experimentally obtained values for

$\frac{\partial A}{\partial \hat{S}_x}$, $\frac{\partial A}{\partial \hat{S}_y}$, $\frac{\partial B}{\partial \hat{S}_x}$, $\frac{\partial B}{\partial \hat{S}_y}$, where S has been non-dimensionalized by k^2/f

and \hat{S}_x , \hat{S}_y are the x- and y-components of baroclinicity, x being in the direction of surface stress. Then

$$\hat{S}_x = \frac{k^2}{f} \frac{\partial u_g}{\partial z} = - \frac{k^2 g}{f^2 T} \frac{\partial T}{\partial y},$$

and

$$\hat{S}_y = \frac{k^2}{f} \frac{\partial v_g}{\partial z} = \frac{k^2 g}{f^2 T} \frac{\partial T}{\partial x}$$

Then for $-90 \leq h/L \leq 90$, (where $h/L = \mu/k$),

$$A = A_o + \left(\frac{\partial A}{\partial \hat{S}_x}\right) \hat{S}_x + \left(\frac{\partial A}{\partial \hat{S}_y}\right) \hat{S}_y = A_o + 0.20 \hat{S}_x - 0.04 \hat{S}_y,$$

$$B = B_o + \left(\frac{\partial B}{\partial \hat{S}_x}\right) \hat{S}_x + \left(\frac{\partial B}{\partial \hat{S}_y}\right) \hat{S}_y = B_o - 0.32 \hat{S}_x + 0.35 \hat{S}_y.$$

With these baroclinic parameters, they used Rossby number similarity to plot the change in the cross-isobaric angle α with respect to the angle between the thermal and geostrophic wind ψ .

Arya and Wyngaard (1975) take a different approach. They suggest that the scale height be the height of the inversion z_i and therefore that A and B are, respectively, universal functions of z_i/L and fz_i/u_* . Then,

$$A_i = \ln \frac{z_i}{z_o} - k \frac{\langle u_g \rangle}{u_*}$$

$$B_i = k \frac{\langle v_g \rangle}{u_*} \text{ sign } f$$

where $\langle u_g \rangle$, $\langle v_g \rangle$ are the vertically averaged boundary layer components of the geostrophic wind, valid for both baroclinic and barotropic atmospheres. When surface geostrophic winds are used, the authors expand their definitions to account for baroclinicity such that

$A = A_i + A'$ and $B = B_i + B'$, where A' and B' are functions of the geostrophic shear, normalized by $(z_i)/u_*$. This formulation differs from Clarke & Hess in that Clarke & Hess use the thermal wind. However, comparisons of results from both methods (with each other and with observations) show quite similar results.

The Clarke & Hess method eliminates the need for determining z_i and the geostrophic shear. However, because of this we must assume temperature gradients to be invariant with height, within our area of interests, for purposes of determining the thermal wind. Since upper air soundings are not always available for a large part of the open ocean, we would prefer a model which does not rely on these soundings in order to calculate the thermal wind from geostrophic wind shear. Thus, the Clarke & Hess method was selected for this model as the simpler of the two methods.

Sensitivity Analysis of No-Slip Model

Stability effects

Stability was computed for the air-sea temperature difference at 5°C increments, holding the geostrophic wind speed constant. This was done for 3 geostrophic winds: 10, 13, and 16 m sec⁻¹. The stability for a given air-sea temperature difference varied for different geostrophic wind speeds, and the cross-isobaric angle α increased with increasing stability. Thus, the model depicts conditions of momentum transfer in the boundary layer. Under stable conditions, the lower boundary increases the turning of the surface winds and decreases the inertial effects. Figure 1 describes the normalized surface wind as a function of stability for each of the above

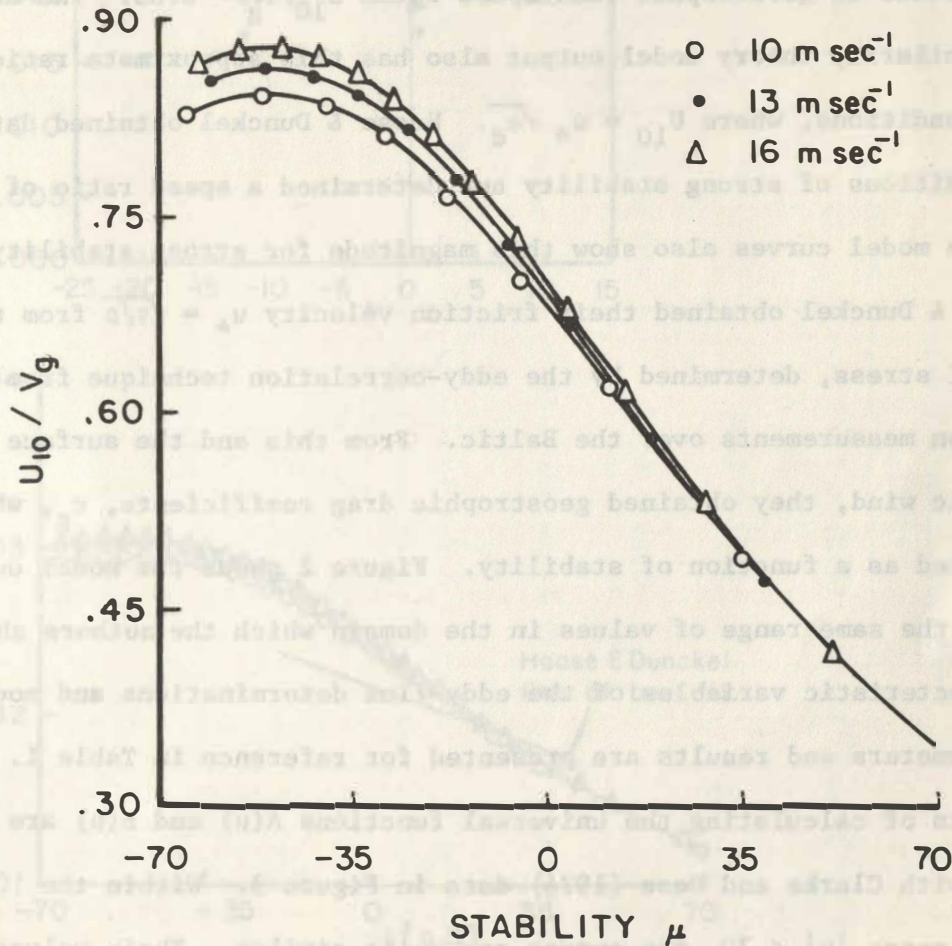


Figure 1. The non-dimensionalized ten-meter wind as a function of stability in a barotropic boundary layer.

geostrophic winds. This shows the surface wind speed increasing with decreasing stability.

Hasse & Dunckel (1974) calculated surface geostrophic winds from 3-hourly pressure observations at German and Danish synoptic weather stations and measured the surface winds over the Baltic. They obtained a mean surface to geostrophic wind speed ratio $U_{10}/V_g = 0.63$. The Rossby number similarity theory model output also has this approximate ratio for neutral conditions, where $U_{10} = u_* \sqrt{c_d}$. Hasse & Dunckel obtained data under conditions of strong stability and determined a speed ratio of 0.39. The model curves also show this magnitude for strong stability.

Hasse & Dunckel obtained their friction velocity $u_* = \sqrt{\tau/\rho}$ from the tangential stress, determined by the eddy-correlation technique from wind fluctuation measurements over the Baltic. From this and the surface geostrophic wind, they obtained geostrophic drag coefficients, c_g , which they plotted as a function of stability. Figure 2 shows the model output as having the same range of values in the domain which the authors show. The mean characteristic variables of the eddy-flux determinations and model input parameters and results are presented for reference in Table I.

Results of calculating the universal functions $A(\mu)$ and $B(\mu)$ are compared with Clarke and Hess (1974) data in Figure 3. Within the stability range $|\mu| \leq 70$, the curves are quite similar. Their values were determined using surface geostrophic winds.

Baroclinic effects

Neutral baroclinic conditions were next investigated. It was desirable to determine the change in cross-isobaric angle, calling the change α' , due to changes of magnitude and direction of the thermal wind.

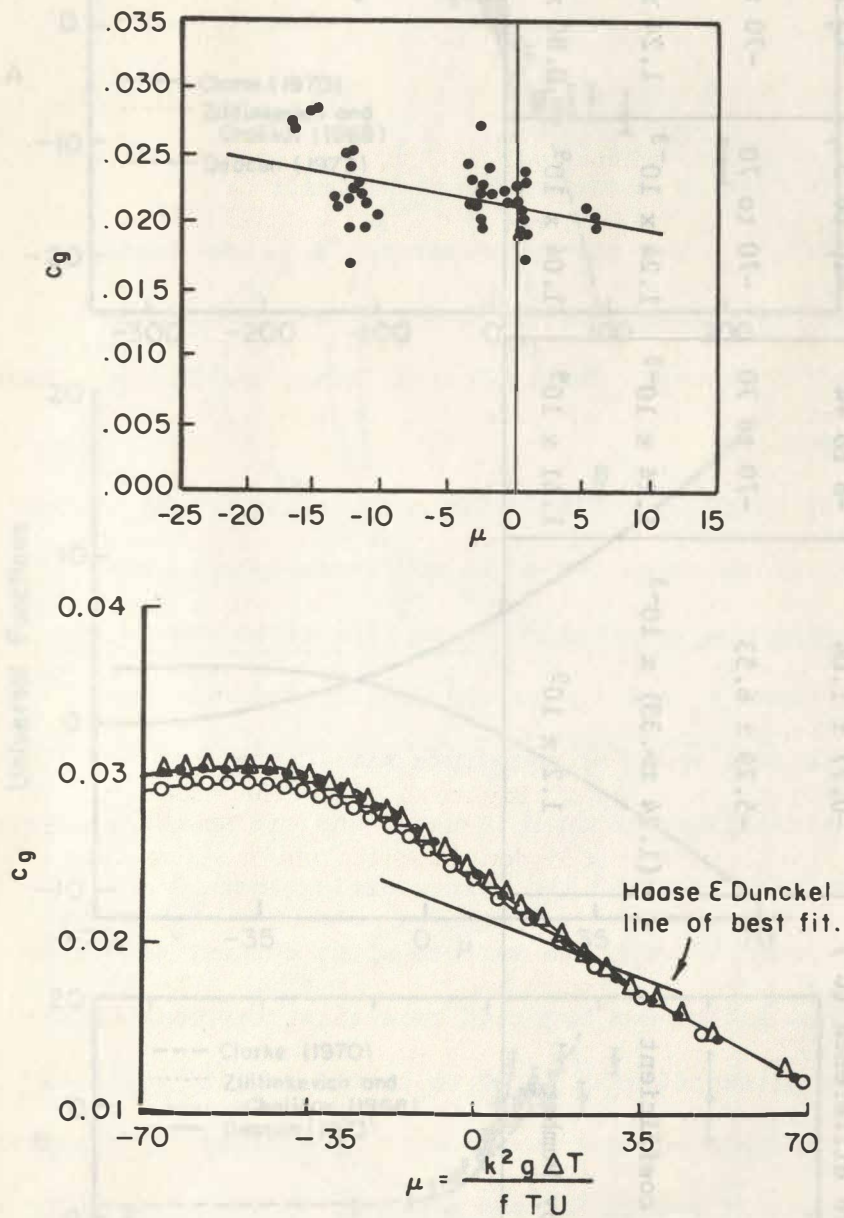


Figure 2. The geostrophic drag coefficient behavior under diabatic conditions. (Upper graph from Haase and Dunkel (1974)).

Table I: Data for Sensitivity Studies

	Hasse & Dunckel data (1974)	Model Input and Results		
		10	13	16
Geostrophic wind speed v_g (m sec ⁻¹)	14.31 ± 3.4			
Air-sea temperature difference (C ^o)	-0.77 ± 1.04	-8 to +4	-10 to 5	-13 to 25
Stability μ	-5.29 ± 6.53	-70 to 70	-70 to 70	-70 to 70
Mean surface drag coefficient	$(1.24 \pm .33) \times 10^{-3}$	1.24×10^{-3}	1.24×10^{-3}	1.24×10^{-3}
Mean surface Rossby Number	1.2×10^9	1.41×10^9	1.04×10^9	0.80×10^9

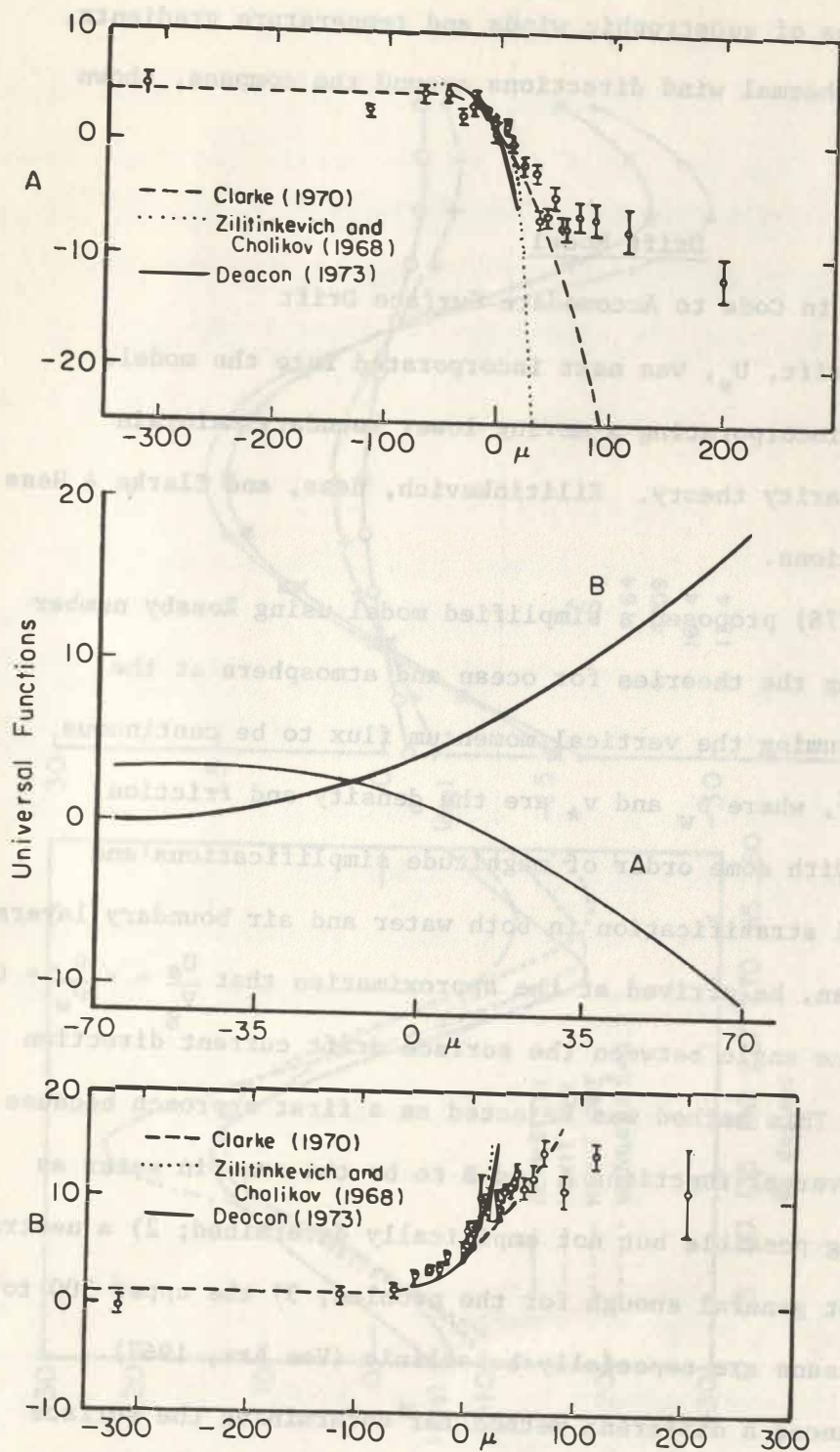


Figure 3. Universal functions A and B as a function of stability. (Top and bottom graphs from Clarke & Hess (1974)).

For various combinations of geostrophic winds and temperature gradients, α' was calculated for thermal wind directions around the compass, shown in Figure 4.

Drift Model

Changes in Code to Accomodate Surface Drift

The sea surface drift, U_s , was next incorporated into the model. It was desirable that incorporating a moving lower boundary maintain the integrity of similarity theory. Zilitinkevich, Hess, and Clarke & Hess offered possible solutions.

Zilitinkevich (1978) proposed a simplified model using Rossby number similarity and matching the theories for ocean and atmosphere at the air-sea interface, assuming the vertical momentum flux to be continuous such that $\rho_w v_*^2 = \rho u_*^2$, where ρ_w and v_* are the density and friction velocity for water. With some order of magnitude simplifications and assumptions of neutral stratification in both water and air boundary layers and a homogeneous ocean, he arrived at the approximation that $\frac{U_s}{v_g} \approx \sqrt{\frac{\rho}{\rho_w}} \approx 0.032$, $\alpha_s \approx \alpha$, where α_s is the angle between the surface drift current direction and the wind stress. This method was rejected as a first approach because 1) he assumed the universal functions A and B to be the same in water as well as air, something possible but not empirically determined; 2) a neutral barotropic case is not general enough for the problem; 3) the upper 500 to 1000 meters of the oceans are especially baroclinic (Von Arx, 1967).

Hess (1974) advanced a different method for determining the surface drift using similarity theory. He also considered the universal functions A and B to be the same for air and ocean and assumed a continuous stress at the interface. He then further simplified the problem by assuming that the

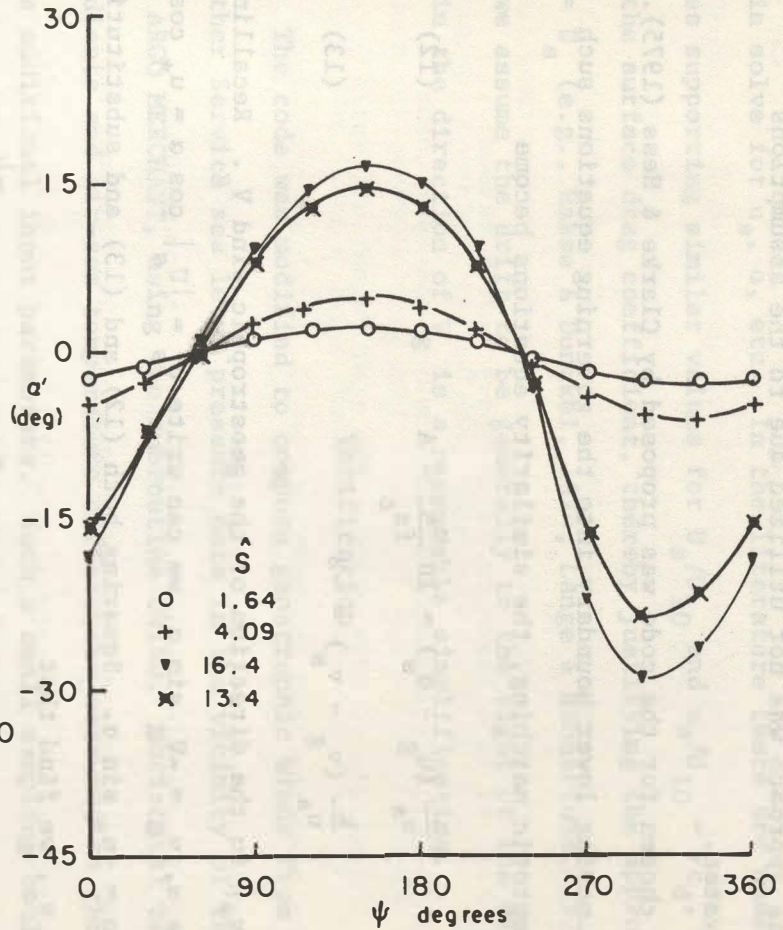
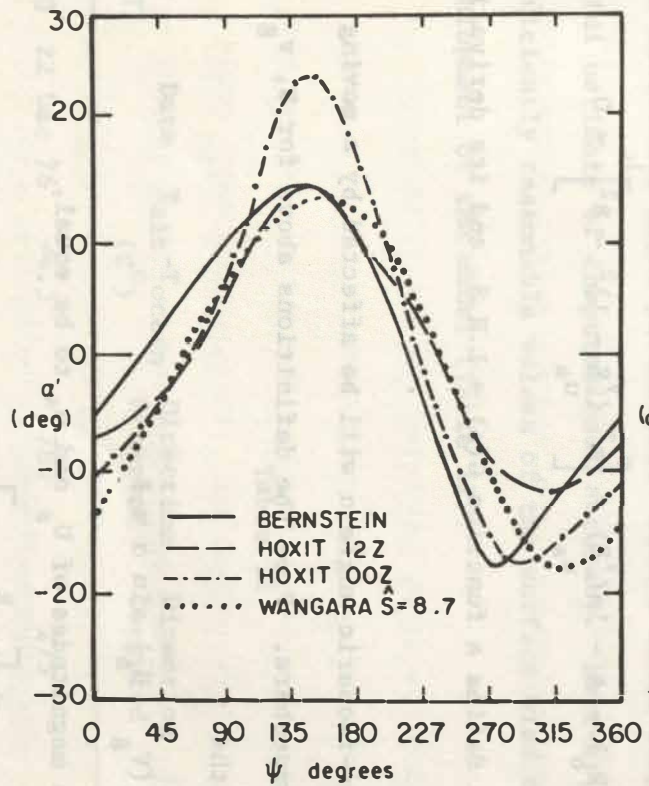


Figure 4. The change in the cross-isobaric angle due to baroclinicity. (Graph on the left from Clarke & Hess (1975). Current model results on the right.)

roughness length in water equals the roughness length felt by the atmosphere. This approach was not utilized due to the assumptions concerning the water.

The method chosen for the code was proposed by Clarke & Hess (1975). They initiate a moving lower boundary into the governing equations such that, after asymptotic matching, the similarity equations become

$$\frac{k}{u_*} (u_g - u_s) = \ln \frac{u_*}{fz_o} - A \quad (12)$$

$$\frac{k}{u_*} (v_g - v_s) = -B \quad (13)$$

where $|U_s| = |u_*|$ in the direction of the geostrophic wind V_g . Recalling that $u_g = V_g \cos \alpha$, $v_g = -V_g \sin \alpha$, we can write $u_s = |U_s| \cos \alpha = u_* \cos \alpha$, $v_s = -|U_s| \sin \alpha = -u_* \sin \alpha$. Squaring both (12) and (13) and substituting for u_g , v_g , u_s , v_s , we find that

$$\ln(R_o) - A - \ln\left(\frac{V_g}{u_*}\right) - \left[k^2 \left(\frac{V_g}{u_*} - 1 \right)^2 - B^2 \right]^{\frac{1}{2}} = 0.$$

Letting $c = 1/c_g$, we can define a function $G(c) = \text{L.H.S.}$ and its derivative $G'(c)$.

Logically, the cross-isobaric angle α will be affected by a moving lower boundary to the atmosphere. From the definitions above for B , v_g , and v_s , it can be shown that

$$\frac{k}{u_*} (V_g - U_s) \sin \alpha = B.$$

Then, again assuming the magnitudes of U_s and u_* to be equal,

$$\alpha = \sin^{-1} \left[\frac{B}{k \left(\frac{V_g}{u_*} - 1 \right)} \right]$$

Using $G(c)$ and $G'(c)$ in the code in place of $F(c_g)$, $F'(c_g)$ we can again solve for u_* , α , etc. In the literature there are numerous cases supporting similar values for U_s/U_{10} and $u_*/U_{10} = \sqrt{c_d}$, where c_d is the surface drag coefficient, thereby justifying the approximation $u_* \approx U_s$ (e.g., Hasse & Dunckel, 1974; Lange & Hühnerfuss, 1978). Then, if we assume the drift to be generally to the right of the wind stress, U_s in the direction of V_g is a reasonable simplification.

Verification

The code was modified to compute geostrophic winds from National Weather Service sea level pressure data in the vicinity of the wreck of the ARGO MERCHANT, using the subroutine GWIND. Horizontal temperature gradients and air-sea temperature differences measured on three occasions were additional input parameters. Such a small sampling could not give a useful estimate of computational accuracy. However, it did yield sufficiently reasonable values of the surface wind to encourage additional development of the model (Table II).

Table II

Hr (EST)	Date	$T_{\text{air}} - T_{\text{ocean}}$ ($^{\circ}\text{C}$)	Direction Observed	Direction Computed	$ U_{10} $ knots Observed	$ U_{10} $ knots Computed
1900	22 Dec 76	-4.3	280	275	15	14.9
0700	23 Dec 76	1	240	223	5	15.8
1900	04 Jan 77	-1.0	320	352	25	10.5

CHAPTER IV

OIL TRANSPORT

The ultimate goal of this research is to apply Rossby number similarity theory to the understanding of stresses on the open ocean and transport of oil slicks on this ocean. The most recent oil spill data available was from the ARGO MERCHANT oil spill, which occurred from the grounding of this vessel off the coast of Massachusetts on December 15, 1976. Many public and private research groups studied this spill, taking various measurements and samples. Our interest here is the meteorological data: wind speed and direction at the wreck site and air and sea temperatures. Flights were also taken over the oil, and position and sometimes speed and direction of oil and water surface were noted.

Because the ARGO MERCHANT studies indicated the oil slick moved in the direction of the wind, the accurate simulation of the wind speed and direction in the general area was considered important. Thence, not only would the slick transport be calculable, but also this model would show in general the ability of Rossby number similarity theory to predict surface winds.

Prediction of winds

A drag coefficient c_d is commonly used to express the relationship

between the mean wind U at a given height and the friction velocity u_* such that $c_d = (u_*/U)^2$. The drag coefficient is assumed to be a function of height z , surface roughness z_o , and stability. For neutral conditions, we often see the familiar logarithmic profile $U = (u_*/k) \ln (z/z_o)$. A number of values have been calculated for c_d , some as a function of wind speed, some of sea surface roughness, and some remaining constant. In the following, c_d refers to the drag coefficient for a 10 meter wind. Hsu (1974) suggested a constant drag coefficient of 1.2×10^{-3} for deep water ocean applications since a large diabatic range does not usually exist over the open ocean. For near neutral conditions, Ruggles (1970) found c_d to be approximately 1.6×10^{-3} for all wind speeds, excluding singularities at 2, 4, and 8.5 m/sec, and Hasse & Dunckle (1974) found $c_d = 1.24 \times 10^{-3}$. SethuRaman & Raynor (1975) also investigated drag coefficients and found that for a given sea surface state, either smooth ($z_o < 0.0015$ cm, $c_d = 0.69 \times 10^{-3}$), moderate (0.0015 cm $\leq z_o \leq 0.015$ cm, $c_d = 1.06 \times 10^{-3}$), or rough ($z_o > 0.015$ cm, $c_d = 1.75 \times 10^{-3}$), the drag coefficient remains constant within that class.

Because observations tend to show a relationship between the surface drift on the ocean and the wind speed at 10 meters as $U_s \approx 0.035 (U_{10})$ (ARGO MERCHANT spill, Torrey Canyon spill, experiments) this would approximate Hasse & Dunckel's coefficient of $\sqrt{c_d} = 0.0352 = (u_*/U_{10})$ if we assume the surface drift to be of approximately the same magnitude as the friction velocity. The test is how closely will the calculated surface wind speed agree with measured data, assuming the magnitude to be determined by $U_{10} = u_*/\sqrt{c_d}$.

The determination of z_o must also be considered. The model used here

utilizes Charnock's (1955) $z_o = \left(\frac{m}{g}\right)u_*^2$, $m = 0.016$ having been verified by Wu (1969), SethuRaman & Raynor (1975), and others.

While there have been some suggestions of an upper bound on the surface roughness over the ocean of 0.02 cm, data from Barger, et. al. (1970) show z_o values greater than 0.1 cm for a "clean" ocean and at least 0.06 cm with sea slicks. From their observations, there are indications, however, of an upper bound for z_o under neutral conditions.

To test these hypotheses about z_o and c_d , the model was run for a variety of cases:

Case 1a: The magnitude of z_o was bounded above by 0.10 cm.

Then, the value of c_d was a step function of z_o such that for $z_o \leq 0.015$, $c_d = 1.24 \times 10^{-3}$, and for $z_o > 0.015$, $c_d = 1.75 \times 10^{-3}$.

Case 1b: The same restriction as Case 1a, but the PBL was assumed to be only diabatic and barotropic.

Case 2: The magnitude of z_o was unbounded. The value of c_d was a step function of z_o such that for $z_o \leq 0.02$ cm, $c_d = 1.24 \times 10^{-3}$, and for $z_o > 0.02$, $c_d = 1.75 \times 10^{-3}$.

Case 3: The magnitude of z_o was bounded above by 0.02 cm, and for all such z_o , $c_d = 1.24 \times 10^{-3}$.

Case 4a: The magnitude of z_o was constant such that $z_o = 0.02$ cm, and $c_d = 1.24 \times 10^{-3}$.

Case 4b: The same restrictions as Case 4a, but the PBL was assumed to be only diabatic and barotropic.

Case 5: The magnitude of z_o was unbounded and $c_d = 1.24 \times 10^{-3}$.

The surface geostrophic wind for 41°N latitude, 69.5°W longitude (the wreck's location) was obtained from sea level pressure surface maps and computed by subroutine GWIND. The horizontal temperature gradient was interpolated for this region from the 700 mb pressure height charts. The

air-sea temperature difference is one indicator of surface stability and was utilized in the computer model to determine the stability parameter μ . During the time period over which the sea level pressures were obtained to compute surface winds and ocean drift, very little air-sea temperature difference information was available. However, synoptics suggested a slightly unstable regime, so the model assumed an air-sea difference of $-3C^{\circ}$. This was an average value from available data.

For wind speed (in knots) and wind direction (in degrees) the mean error, root mean square of the error, mean absolute error, and estimates of simulation skill are shown in Table III. The error was determined as the difference between the computed and observed parameter; computed via Rossby number similarity and observed at the ARGO MERCHANT site. The observed parameter was either the hourly observed datum at time t or the mean of three hourly observed data, centered about time t . The skill estimates were determined from NWS criteria (Grose & Mattson, 1977). By NWS experience, a wind direction forecast that verifies within 30° is considered as excellent and within 60° as good to excellent; wind speed error of 5 knots as excellent, 10 knots as good to excellent. While these computations were not forecasts but rather simulations, these criteria can give us an estimate of the model's usefulness.

Results of these comparisons imply that all the above cases for determining surface winds yield reasonable numbers. Thus, for a given problem, the user must decide what kind of error values are acceptable and what level is necessary and/or sufficient to yield useful output. It would appear, from the root mean squares, that the calculation of

TABLE III. Statistical Results of Model Cases*

Case	1a	1b	2	3	4a	4b	5
$(\overline{U_c - \overline{U}})$	1.30	-1.26	1.44	2.38	3.23	-1.15	4.05
$\sqrt{(\overline{U_c - \overline{U}})^2}$	6.67	5.85	6.57	7.04	7.39	8.39	8.68
$ \overline{U_c - \overline{U}} $	4.90	4.56	4.94	5.05	5.16	6.63	5.99
Excellent U_c	16	17	15	17	17	11	15
Good U_c	5	5	6	4	4	7	5
$(\overline{D_c - \overline{D}})$	16.71	15.44	16.54	16.87	16.68	14.99	16.20
$\sqrt{(\overline{D_c - \overline{D}})^2}$	28.06	26.90	27.96	27.82	28.10	27.43	27.67
$ \overline{D_c - \overline{D}} $	23.67	23.03	23.50	23.64	23.65	23.65	23.19
Excellent D_{ca}	16	17	16	16	16	17	16
Good D_{ca}	7	6	7	7	7	6	7
$(\overline{U_c - \overline{U}})$	1.25	-1.30	1.39	2.34	3.19	-1.20	4.00
$\sqrt{(\overline{U_c - \overline{U}})^2}$	7.10	6.67	7.04	7.48	7.77	9.26	8.92
$ \overline{U_c - \overline{U}} $	5.44	5.12	5.51	5.74	5.94	7.51	6.66
Excellent U_c	12	15	11	13	16	9	12
Good U_c	9	6	10	7	4	8	8
$(\overline{D_c - \overline{D}})$	18.53	17.25	18.35	18.68	18.49	16.81	18.02
$\sqrt{(\overline{D_c - \overline{D}})^2}$	31.22	29.93	31.17	31.03	31.27	30.55	30.89
$ \overline{D_c - \overline{D}} $	27.11	25.34	27.12	26.98	27.02	25.73	26.82
Excellent D_{co}	13	14	13	13	13	14	13
Good D_{co}	10	8	10	10	10	9	10

*Computed surface wind speed (U_c) and direction (D_c) are compared with observed wind (U , D) and three-hour mean observed winds (\overline{U} , \overline{D}). Wind speed is in knots and direction is in degrees. The overbar indicates a mean quantity derived as $1/n \sum$ (quantity), $n = 23$. Excellent and good forecast speed and direction refer to the number of times the absolute value of the difference of (calculated-mean observed), subscripted ca, or difference of (calculated-observed), subscripted co, were in the good and excellent range used by NWS.

U_{10} with no temperature advection yields the smallest deviation from observed. However, this method consistently underestimates the observed speeds. The next smaller root mean square value for wind speed error was derived from case 1a. The surface roughness parameter was given a least upper bound of 0.1 cm with the surface drag coefficient as a function of z_0 . This method yielded the smallest mean error in comparison with instantaneous wind speed data. The output from these two runs (u_* , U_{10} , direction) were used as input into the oil spill movement model and movement results, to be discussed under Transport of Oil, were compared to an observed slick.

Transport of Oil

The movement of oil on the ocean involves the spreading and transport of the oil. In an instantaneous spill there is initially a gravity spread with viscosity being important in limiting its extent. After a few hours, the slick's thickness will decrease to approximately 1 mm and from then on, horizontal turbulent diffusion becomes the dominant factor in spreading (Ichiye, 1973). After a time, an emulsion of oil and water forms, and thereafter, gravity effects are negligible, and the oil is transported as a passive mass by surface forces: winds, currents, tides, and flows caused by surface slope and density gradients. While both spreading and transport are important, it was decided to simulate the transport of the centroid of oil under conditions of a continuous spill, neglecting for now the effects of spreading.

Texas A & M investigators estimate the transport of oil on the sea surface as the vector sum of the water current and 3.1% of the wind (Wesly, et. al., 1972). Five models were used to forecast or hindcast

the movement of the oil spilled from the ARGO MERCHANT (Grose & Mattson, 1977). These all determined advection by currents and a differential oil-to-water velocity, differing in choices of sources of wind and currents and of wind effects (or wind factor). This wind factor was assumed to incorporate the effects of Ekman currents, Stokes drift, and momentum transfer by waves.

The wind sources for the NOAA study (Grose & Mattson, 1977) were either observed on site and NWS forecasts or climatological winds. Wind factors for 4 of the models were 3% to 3.5% of the wind speed at 0° , 15° , or 20° to the right of the wind. This wind factor is quite close to the value of the drag coefficient utilized in this model. Their observed wind factor averaged out to 3.56% over a 4-day period, quite close to the 3.5% value used in their models.

The United States Geological Survey (USGS), in studying the spill, found that no conclusion could be drawn about the accuracy of prediction using a 0° or 20° drift angle. Measurements of the oil speed relative to water and wind showed the oil moving in the same direction as the wind at a speed, relative to the surface current, of 1.1% of the wind speed. That is, the oil slicks would overtake a dye pill which was assumed to move with the surface drift.

With these methods and observations in mind, for simplicity's sake, the oil was moved in the direction of the wind and with the speed of the surface drift plus 1.1% of the wind speed. The movement was simulated using winds and surface drift calculated by Rossby number similarity theory and with wind observations at the ARGO MERCHANT site, with surface drift computed as a function of the drag coefficient. The

oil was assumed to be emitted continuously from the ARGO MERCHANT. Every 12 hours the slicks would be moved by a vector calculated to be the distance the oil would move in 12 hours given a steady wind.

Both of these computations overestimated the longitudinal (east-west) drift of the slick after a 13 day time period (December 15 to December 27, 1976). However, when oil was constrained to move with the speed of the drift alone, the calculated path from model output (case 1a) closely resembled the mean observed path, longitudinally and latitudinally. The observed 12 hour wind data, as input, had underestimated the latitudinal extent. Case 1b output was also utilized as input to the oil slick movement code, and showed the observed oil slick to be longitudinally underestimated and greatly overestimated in its southern extent (Figure 5). The only difference between cases 1a and 1b was that 1b was barotropic. This suggested that baroclinicity was a significant factor in the model. The importance of baroclinicity was confirmed from the results of cases 2 through 5. Except for 4b, cases 2 through 5 closely resembled the observed oil path. Case 4b was the other case which was barotropic.

Discussion

Case 1a data slightly overestimated the east-west and north-south extent of the slick and followed the centroid better than the other two cases discussed. From the vantage point of risk estimation, a slight overestimation of total extent would be better than large overestimation in one direction and large underestimation in the other. Also dissipative effects have not yet been incorporated into the model. These effects would tend to decrease the computed progress of the slick, thereby modifying slight overestimations. However, they would negatively bias an already

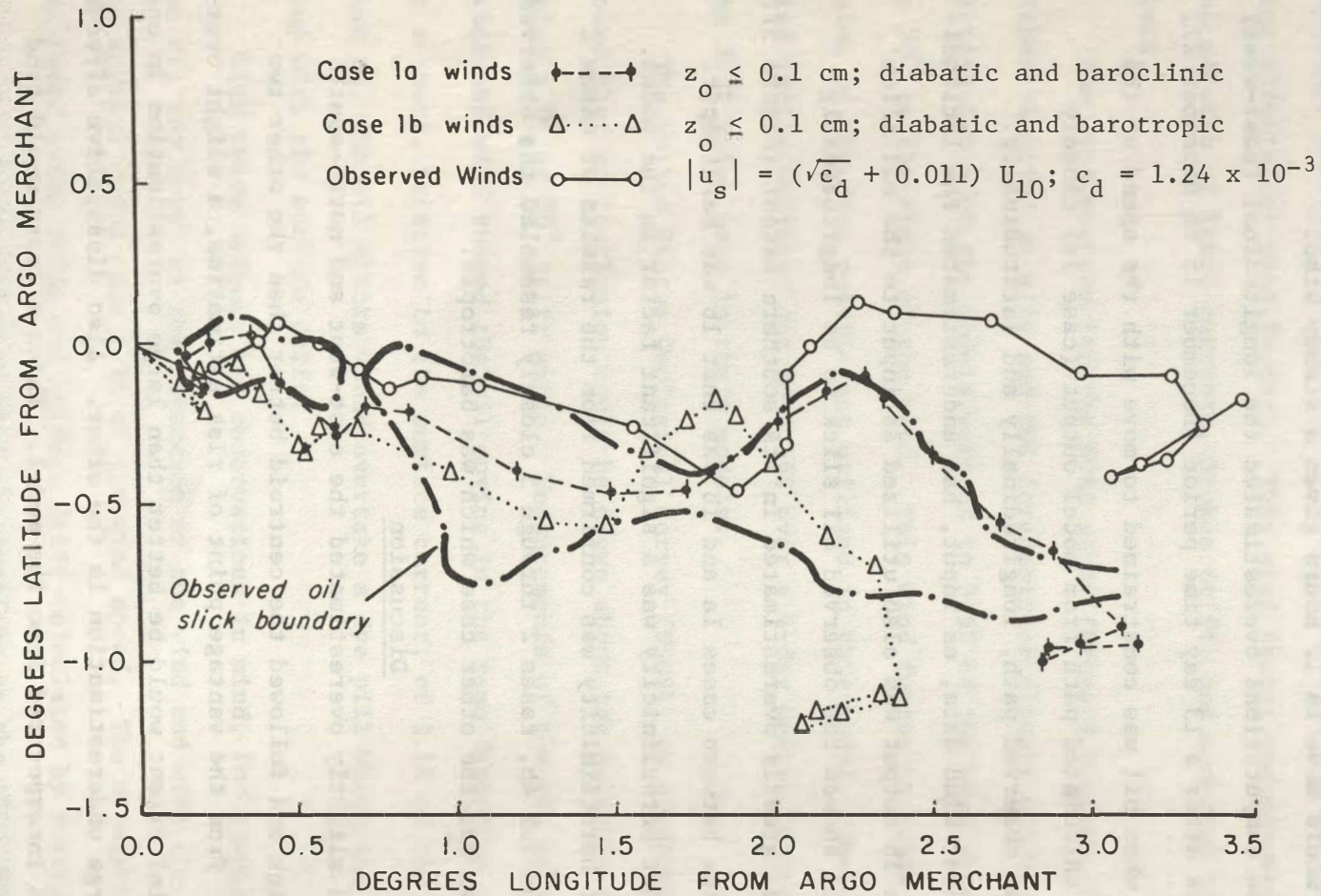


Figure 5. Location of the ARGO MERCHANT oil plume on 27 December 1976 compared with the plume centerlines calculated from observed winds and from model winds for Cases 1a and 1b.

underestimated slick.

Recall, now, that the slick movement calculated from observed winds was based on the premise that the slick really did move at the speed of the sum of surface current and 1.1% of wind speed. If the latter parameter were not utilized in determining the oil movement, the southern extent of oil would have been even more in error compared with the observed slick. Because case 1a simulates the oil movement so well, one could question the accuracy of the observed wind speed and direction measurements obtained near the ARGO MERCHANT during this time. Perhaps there is even less error between the winds generated by Rossby number similarity theory and the actual winds than is indicated in Table III.

One could agree that the surface current magnitude computed from observed winds could be improved with a variable drag coefficient such as utilized by case 1. If the aerodynamic roughness exceeded the criteria for moderate seas, a larger c_d could have been used. This would increase the drift magnitude but also the east-west oil boundary error. Because the roughness cannot be determined by a surface wind speed alone, any improved drift by this method is questionable.

When there is oil on the ocean, we are considering a complex set of events. A thin slick is being acted upon by the atmosphere above and the ocean below. Near a coastline, complications continue to mount. Land mass and ocean bottom effects are experienced by the ocean. Established currents and tides affect the water's motion. Meteorologically, mesoscale effects such as a land-sea breeze are a possibility. These complications were basically neglected in the model. This can be justified if we assume there exists more homogeneity over the open ocean, where the model is

intended for use.

Nevertheless, the verification for this model was an oil slick emanating from the ARGO MERCHANT wreck. This wreck was located only 29 nautical miles southeast of Nantucket Island, Massachusetts. Thus tides and currents, along with diffusion, probably did play a part in the oil slick's eventual expanse. The United States Coast Guard (USCG) Research & Development Center determined that while tides and winds would control the movement of the oil over the short term (24 hours), the wind would dominate its progress over the long run (NOAA, 1977). This could explain the favorable comparison of case 1a simulation to the observed slick.

Land-sea breezes would account for discrepancies in the measured wind from computed wind which were not explainable from large scale synoptics. It must be remembered that the forces determining the flow field in this model are pressure and frictional. Centripetal forces have thus been excluded from outright consideration. Sometimes, the surface wind under analysis from December 15 to December 27 was gradient (curved) flow. This could also affect observed wind values.

CHAPTER V

CONCLUSION

This study was undertaken to determine the validity of utilizing Rossby number similarity theory to calculate surface winds and movement of an oil slick's centroid over the open ocean. Rossby number similarity necessitated assumptions of a neutral, steady state, horizontally homogeneous atmosphere with no heat transfer. This simple model was then expanded to encompass diabatic and baroclinic conditions and later a moving lower boundary. The model has limitations, however, involving these latter conditions. The stability factor μ is bounded by ± 70 , beyond which the model will not converge. Likewise, large horizontal temperature gradients (greater than $4^{\circ}\text{C}/100\text{ km}$) will require larger geostrophic wind speeds to effect convergence. The implication is that Rossby number similarity does not adequately describe an environment where the thermal wind is the dominant driving mechanism. This is to be expected when one recalls that the pressure, coriolis, and frictional forces are the basis of the theory. Under steady state conditions, one would not often expect large horizontal temperature gradients in middle latitudes over the open ocean.

Of the five variables in the Rossby number similarity model, V_g , f , z_o , μ , and \hat{S} , the surface roughness z_o and the baroclinicity \hat{S} were varied in an attempt to obtain an oil slick path from the calculated friction velocity

u_* and surface cross isobaric angle α . The input data was the calculated surface geostrophic wind, calculated baroclinicity, and approximated diabaticity. The oil slick path calculated using Rossby number similarity theory was obtained by moving the oil in the computed direction of the surface wind with the speed of the friction velocity u_* . Seven cases were run to calculate paths. Within the range of the roughness parameter considered, the results show that variations in baroclinicity are more significant than any reasonable variations in roughness in reproducing the observed oil slick path.

The drag coefficient c_d was also varied in the seven cases in this study. This coefficient was utilized to obtain information from the u_* calculated in the model. This information was then compared with observed data. Assuming a constant drag coefficient tended to result in slightly larger errors. However, for all seven cases, the mean error between calculated and mean observed wind speeds did not exceed 4.1 knots, and the direction difference error did not exceed 17° . It can therefore be concluded that this model can be useful in determining the surface winds over the open ocean.

Much work remains to be done. Spreading has been neglected, and refinements to include evaporation, dissolution, and dispersion should enhance the oil slick model's predictive capability. Results from the Rossby number similarity theory model have been shown to be useful input for an oil slick model.


```

PROGRAM THE9IB(INPUT,TTY,CARDS,OUTPUT,TAPE5=CARDS,TAPE6=OUTPUT,
1 TAPE8)
DIMENSION ITITLE(6)
REAL LRMA,K,LL,K2,LC,MU,L,KV
COMMON/G/ IDMAX,JDMAX,XLAT,COR(4),TWRD(6,4),DX(4),DY(4),
1 RR,ICMAX,JCMA,OMEGA,SLP(6,4),PHI0(6,4),VG0(6,4)
DATA DX/8539800.,8413900.,8205500./,DY/11104750.,11106690./
COMMON/W/ RF,VG,ZI, SX0,SY0,A0,B0,PHI1,DELTA,EP8,GM,RGM,
1 K2,G,ITER1,ITER2,ITER3,DELHT,DTOA,T,K,RCD,IDEBUG
COMMON/WO/ U,THETA,USTAR
DIMENSION XNIL(34),YOIL(34)
COMMON AVU(48),AVD(48),AVFR(48),AVGG(48),USTR(48),FI(48)
KASE=0
LMX= 121
X00=Y00=0.0
NLIN=0
DELTA= 1.0E-2
N=0
NSLICK=0
ITER1=ITER2=ITER3=20
NTIME=0
CC=0.016
K=0.4 S G=981.0 S RHO=1.2E-3
GM= G/CC S RGM= 1.0/GM
K2= K*K
RR= 1000./RHO
ZI= 0.01
SX0=SY0=0.0
A0= 1.1 S B0= 4.3
EP8=1.0E-05
OMEGA=7.292E-05
DATA IN CGS SYSTEM
C INPUT INITIAL VALUES OF GEOSTROPHIC WIND VG/,SFC. ROUGHNESS ZR
C SHEAR SX AND SY, SIMILARITY THEORY A0 AND B0,
C THE HORIZONTAL TEMP. GRADIENT AND ANGLE RELATIVE TO SFC.STRESS,
C HEAT FLUX, AND TEMP T
C PHI1 IS ANGLE OF TEMP GRADIENT VECTOR FROM COLD TO WARM WHEN COMPUTING
C FROM SYNPTIC MAPS. LATER MADE RELATIVE TO GEOSTROPHIC WIND AS P08
100 IF(KASE.EQ.0) GO TO 3
READ(5) (AVU(I),I=1,204)
DO 2 I=1,34
IF(MOD(I+1,2).EQ.1) GO TO 1
READ(5,1006) IVG,DELHT,U1,T,DTOA,CD,XLAT,
1 IDEBUG,IDMAX,JDMAX
XLAT=XLAT+1.
1,VG= AVGG(I)
PHI1= FI(I)
C GEOSTROPHIC WINDS WILL NOT BE CALCULATED FROM SLP,
FF = 2.0*OMEGA*SIN(XLAT*0.01745)
RF= 1.0/FF S RCD= 1.0/SQRT(CD)
CALL WIND,

```



```

2 CONTINUE
  STOP
C   BELOW COMPUTES GEOSTROPHIC WINDS WITH CALL TO GWIND
3 READ(5,1006) IVG,DELHT,PHI1,T,DTOA,CD,XLAT,IDEBUG,IDMAX,JDMAX
  IF(IVG.LT.0) GO TO 1999
  PHI0(1,1)= PHI1
  CALL GWIND
C
4 CONTINUE
  READ(5,1011) ITITLE
C
  WRITE(6,1005) ITITLE
  WRITE(6,1007) IVG,DELHT,PHI1,T,DTOA,CD,XLAT,IDEBUG,IDMAX,JDMAX
C
  ROM=0.3      SHM= 0.
  RCD= 1.0/SQRT(CD)
5 CONTINUE
  DO 999 J=2,JCMAX
  FF=COR(J)    $   RF= 1.0/FF
  USAVE=0.    $   DSAVE=0.
  DO 998 I=2,ICMAX
  PHI1= PHI0(I,J)
  VG= VG0(I,J)
  IF(VG.LE.500.) DELHT=1.2E-8
  CALL WIND
  DIR= TWRD(I,J)+THETA
  TEMP= 270.-DIR*57.3
  FROM=AMOD(TEMP,360.)
  WRITE(6,1008) FROM,VG,PHI1
  NTIME=NTIME+1
  USTR(NTIME)=USTAR $ FI(NTIME)=PHI1
  AVGG(NTIME)=VG $ AVFR(NTIME)=FROM
  AVU(NTIME)=U $ AVD(NTIME)= DIR
998 CONTINUE
999 CONTINUE
  GO TO 100
1999 CONTINUE
  WRITE(8) AVU,AVD,AVFR,AVGG,USTR,FI
C
1005 FORMAT(///,6A10)
1006 FORMAT(I5,7PF5.0,0P,3F5.0,3PF5.0,0PF5.0,3I3)
1007 FORMAT(* IVG=*,I5,5X,* DELHT=*,E9.2,5X,*PHI1=*,F5.0,5X,*T=*,
  1F5.0,5X,*DTOA=*,F5.2/,* DRAG COEF FOR U10=*,E9.2,5X,*LATITUD=*,
  2 F5.1,5X,*DEBUG FLAG=*,I1,5X,*IDMAX=*,I3,5X,*JDMAX=*,I3)
1008 FORMAT(1H+,50X,*, FROM=*,F5.0,*, VG=*,F6.1,*, PHI1=*,F5.0)
1009 FORMAT(1H ,*TOTAL NUMBER OF SLICK POINTS=*,I4,* X,Y *,
  1*COORDINATES IN METERS FROM ORIGIN FOLLOW*/,
  2 (6(1X,1H(,E9.2,1H,,E9.1,1H) ))
1011 FORMAT(6A10)
  END

```

```

SUBROUTINE WIND
COMMON/W/ RF, VG, ZI, SX0, SY0, A0, B0, PHI1, DELTA, EPS, GM, RGM,
1 K2, G, ITER1, ITER2, ITER3, DELHT, DTOA, T, K, RCD, IDEBUG
COMMON/WO/ U, THETA, USTAR
REAL K2, K, LRMA, MU
F(C) = LRMA - ALOG(C) - SQRT(K2*(C-1.)*(C-1.) - B2)
FP(C) = -1.0/C - K2*C/ SQRT(K2*(C-1.)*(C-1.) - B2)
AA(C) = A0 - 0.10*C = 0.001*C*C
BB(C) = B0 + 0.13*C + 0.001*C*C
Z0 = ZI      S      SX = SX0      S      SY = SY0
A = A0      S      B = B0
PHI = PHI1 * 0.01745
RVG = 100/VG
B2 = B*B
USTAR = SQRT(Z0*GM)
X1 = VG/USTAR
ITER = 0
IBFLG = 1
IF(T.LE.0.0 .OR. ABS(DELHT).GT.1.0E-20) IBFLG = 2
C THIS IBFLG = 2 IMPLIES A, B WILL NOT BE COMPUTED AS FCN
C OF MU ONLY
IF(T.LE.0.0) GO TO 100
AMU = K2*G*OTOA*RF/T
SS = K2*G*RF*RF/T
90 U = USTAR*RCDT
IF(Z0.GT.0.015) U = USTAR/SQRT(1.75E-03)
C FOR ROUGH SEA STATE, CHANGE DRAG COEF.
C
MU = AMU/U
A = TAA(MU)
B = BB(MU)
B2 = B*B
C BAROTROPIC CASE
100 RO = VG*RF/Z0
LRMA = ALOG(RO) - A
X = X1
C ITERATE ON (VG/USTAR)
DO 20 I = 1, ITER1
X1 = X - F(X)/FP(X)
Y = F(X1)
IT = I
IF(ABS(X1 - X).LT. EPS ) GO TO 30
20 X = X1
WRITE(6, 1010) ITER1
GO TO 999
30 IF(IDEBUG.EQ.1) WRITE(6, 1020) IT, X1, Y
C COMPUTE USTAR
USTAR = VG/X1
Z1 = Z0
Z0 = RGM*USTAR*USTAR
C
C UPPER BOUND ON Z0
IF(Z0.LT.0.10) GO TO 31
Z0 = Z1
GO TO 200
31 CONTINUE
ITER = ITER + 1

```

```

IF( ABS(Z1-Z0).LT.1.0E-4) GO TO 200
IF(ITER.LT.ITER2) GO TO (90,100) IBFLG
WRITE(6,1030)ITER,USTAR,R0,Z0,Z1
C
C CONVERGES
C CLACULATE THETA
C 200 THETA= ASIN(B*USTAR/(K*VG))
200 THETA= ASIN(B/(K*(X1-1.0)) )
IF(ITER.EQ.0) ALPHA=THETA
THETA= THETA*57.3
IF(IDEBUG.EQ.1) WRITE(6,1040) USTAR,R0,Z0,THET
IF(ABS(DELHT).LT.1.0E-20) GO TO 980
C
C BAROCLINIC CASE
C PSI= PHI-THETA
C COMPUTE X, Y COMPONENTS OF TEMP. GRADIENT ALIGNED WITH SFC. WIND
DTX= DELHT*COS(PHI)
DTY= DELHT*SIN(PHI)
C COMPUTE SX,SY
SXH=-SS*DTY
SYH= SS*DTX
IF(ABS(SXH-SX).LT.DELTA.AND.ABS(SYH-SY).LT.DELTA) GO TO 200
C COMPUTE MU,A,B
U= USTAR*RCD
IF(Z0.GT.0.015) U= USTAR/SQRT(1.75E-03)
C FOR ROUGH SEA STATE, CHANGE DRAG COEF.
MU= AMU/U
A=AA(MU)
B=BB(MU)
A= A+0.20*SXH-0.04*SYH $ B= B-0.32*SXH+0.33*SYH
203 ITER=ITER+1
IF(IDEBUG.EQ.1) WRITE(6,1000) U,MU,A,B
IF(ITER.GT.ITER1) GO TO 990
B2=B*B
SX=SXH $ SY=SYH
ITER=0
GO TO 100
250 SH=SQRT(SXH*SXH+SYH*SYH)
ALPHAP= 57.3*(THETA-ALPHA)
FORK= PHI1+90.0
IF(IDEBUG.NE.2) GO TO 999
WRITE(6,1035) ALPHAP,FORK
WRITE(6,1050)SXH,SYH,SH
980 WRITE(6,1040) USTAR,R0,Z0,THET
WRITE(6,1000) U,MU,A,B
GO TO 999
990 WRITE(6,1070)A,B,PHI1
WRITE(6,1060)SX,SY,SXH,SYH
999 CONTINUE
1000 FORMAT(1H ,*U** ,E10.2,* , MU** ,E10.2,* , A** ,F7.2,* , B** ,F7.2)
1010 FORMAT(23H#FAILED TO CONVERGE IN ,I3,11H ITERATIONS)
1020 FORMAT(14H CONVERGES IN ,I3,16H ITERATIONS, X1= ,F11.7,
1 14H FOR U*/VG, Y= ,F11.6)
1030 FORMAT(1H ,* SFC. ROUGHNESS ITERATIONS** ,I3,* USTAR** ,F10.3,
1 * , ROSSBY NO. ** ,E10.2,* , SFC. ROUGHNESS** ,2E10.1)
1035 FORMAT(* ALPHA PRIME** ,F9.3,* , ANGLE OF THERMAL WIND** ,F9.3)
1040 FORMAT(* USTAR** ,F10.3,
1 * , ROSSBY NO. ** ,E10.2/* SFC. ROUGHNESS** , E10.1,* , THETA** ,F6.2)
1050 FORMAT(1H ,* SXH** ,E10.2,* , SYH** ,E10.2,* , SH** ,E10.2)
1060 FORMAT(* SX,SY,SXH,SYH** ,4E15.3)
1070 FORMAT(* A AND B FAILED TO CONVERGE, A,B** ,2E15.3,* , PHI** ,F5.1)
RETURN
END

```



```

SUBROUTINE GWIND
COMMON/G/ IDMAX,JDMAX,XLAT,COR(4),TWRD(6,4),DX(4),DY(4),
1 RR,ICMAX,JCMAX,OMEGA,SLP(6,4),PHI0(6,4),VG0(6,4)
JCMAX=JDMAX-1 % ICMAX=IDMAX-1

```

```

PHI1=PHI0(1,1)

```

```

C INPUT PRESSURES

```

```

DO 5 J=1,JDMAX

```

```

5 READ(5,103) (SLP(I,J),I=1,IDMAX)

```

```

C DO 20 J=2,JCMAX

```

```

XLAT=XLAT+1.0

```

```

COR(J)=2.0*OMEGA*SIN(XLAT*0.01745)

```

```

JP1=J+1 % JM1=J-1

```

```

RDX=0.5/DX(J) % RDY=1./(DY(JM1)+DY(J))

```

```

COEFX=RR*RDX/COR(J) % COEFY=-RR*RDY/COR(J)

```

```

DO 10 I=2,ICMAX

```

```

GV=COEFX*(SLP(J+1,J)-SLP(I=1,J))

```

```

GU=COEFY*(SLP(I,JP1)-SLP(I,JM1))

```

```

VG0(I,J)=SQRT(GV*GV+GU*GU)

```

```

TWRD(I,J)=ATAN2(GV,GU)

```

```

TEMP=270.0-TWRD(I,J)*57.3

```

```

FROM=AMOD(TEMP,360.)

```

```

PHI0(I,J)=AMOD(FROM-PHI1+360.0,360.0)

```

```

10 CONTINUE

```

```

20 CONTINUE

```

```

C 103 FORMAT(12F6.1)

```

```

RETURN

```

```

END

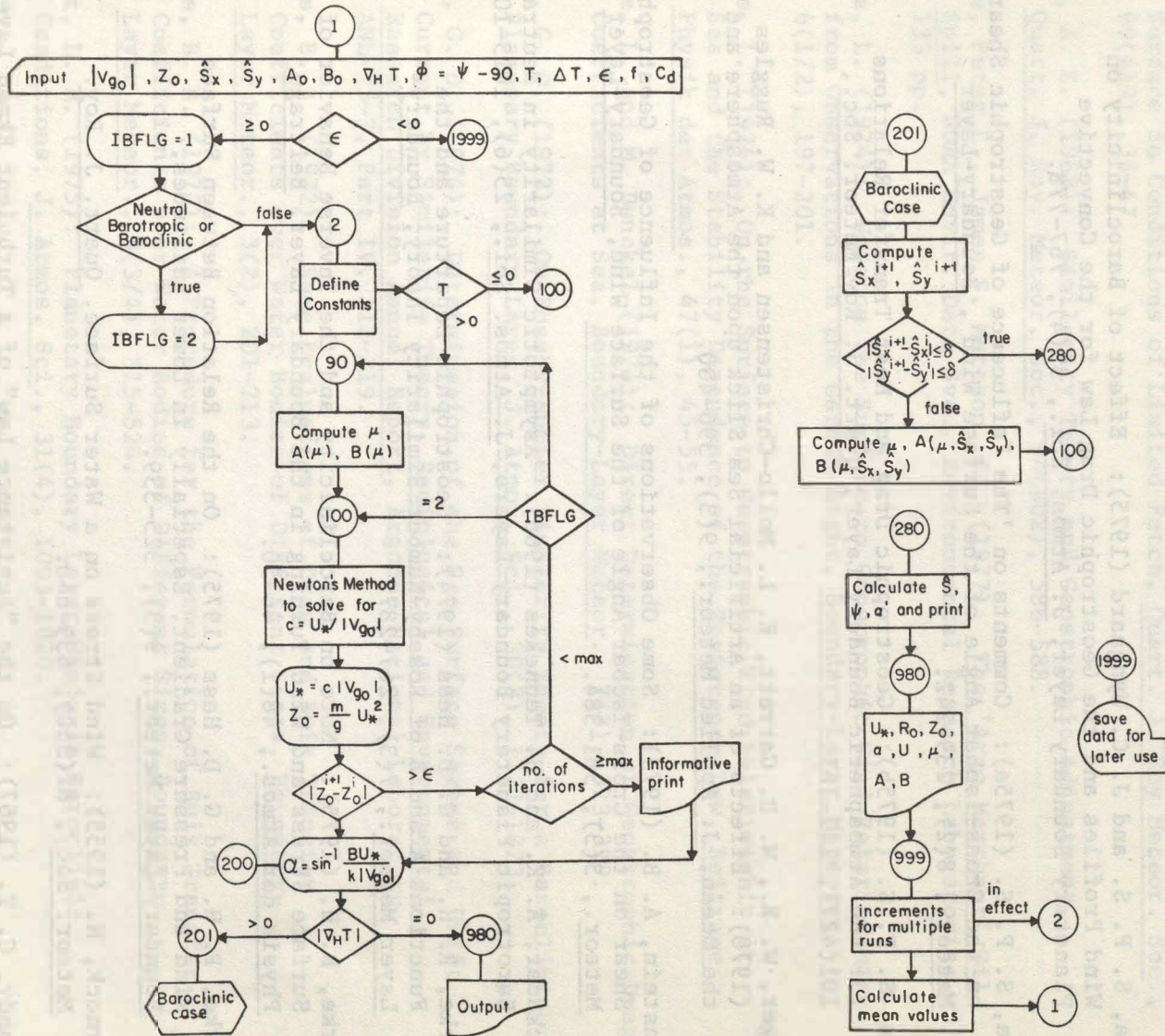
```

```

PROGRAM MOVEIT(INPUT,OUTPUT,TTY,TAPE6=OUTPUT,TAPE8,TAPE9)
COMMON AVU(48),AVD(48),AVF(48),AVGG(48),USTR(48),FI(48),
1 XOIL(24),YOIL(24)
XMAX=YMAY=0,
XMIN=YMAY=0,
CD2= SQRT(1.24E-03)
J=0
READ(9) (AVU(I),I=1,200)
DO 10 K=1,24
IF(K.EQ.3) GO TO 10
J=J+2  S  JM1=J-1
AVU(K)= 0.005*(AVU(J)+AVU(JM1))
AVD(K)= 0.5*(AVD(J)+AVD(JM1))
USTR(K)= 0.005*(USTR(J)+USTR(JM1))
10 XOIL(K)=YOIL(K)=0.
AVU(3)=15.  S  AVD(3)= -150.*0.01745  S  USTR(3)=CD2*AVU(3)*.5144
DO 50 N=1,24
OILV= USTR(N)
DIST= OILV*3600.
XO= DIST*COS(AVD(N))*12./84139.
YO= DIST*SIN(AVD(N))*12./111050.
DO 20 NN=1,N
XOIL(NN)= XOIL(NN)+XO
YOIL(NN)= YOIL(NN)+YO
IF(N.LT.24) GO TO 20
XMIN= AMIN1(XMIN,XOIL(NN))
YMIN= AMIN1(YMIN,YOIL(NN))
XMAX= AMAX1(XMAX,XOIL(NN))
YMAX= AMAX1(YMAX,YOIL(NN))
20 CONTINUE
50 CONTINUE
WRITE(6,1001) XMIN,XMAX,YMIN,YMAX
1001 FORMAT(1X,*XMIN=*,E10.2,*, XMAX=*,E10.2,*, YMIN=*,E10.2,
1 *, YMAX=*,E10.2)
WRITE(8) XOIL,YOIL
END

```


Define $F(c) = \ln R_0 - A + \ln(c) - \sqrt{k^2/c^2 - B^2}$, and $F'(c)$



REFERENCES

- Arya, S. P. S. and J. C. Wyngaard (1975): Effect of Baroclinicity on Wind Profiles and the Geostrophic Drag Law for the Convective Planetary Boundary Layer, J. Atmos. Sci., 32(4), 767-778.
- Arya, S. P. S. (1975a): Comments on 'The Influence of Geostrophic Shear on the Cross-Isobar Angle of the Surface Wind', Boundary-Layer Meteor., 8(2), 239-242.
- Arya, S. P. S. (1975b): Geostrophic Drag and Heat Transfer Relations for the Atmospheric Boundary Layer, Quart. J. Roy. Meteor. Soc., 101(427), 147-161.
- Barger, W. R., W. D. Garrett, E. L. Mollo-Christensen and K. W. Ruggles (1970): Effects of an Artificial Sea Slick upon the Atmosphere and the Ocean, J. Applied Meteor., 9(3), 396-400.
- Bernstein, A. B. (1973): Some Observations of the Influence of Geostrophic Shear on the Cross-Isobar Angle of the Surface Wind, Boundary-Layer Meteor., 3(3), 381-384.
- Blackadar, A. K. and H. Tennekes (1968): Asymptotic Similarity in Neutral Barotropic Planetary Boundary Layers, J. Atmos. Sci., 25(6), 1015-1020.
- Clarke, R. H. and G. D. Hess (1974): Geostrophic Departure and the Functions A and B of Rossby-Number Similarity Theory, Boundary-Layer Meteor., 7(3), 267-287.
- Clarke, R. H. (1975): Note on Baroclinicity and the Inverse Behavior of Surface Stress and Wind Turning in the Boundary Layer, Beitrag Physik der Atmos., 48(1), 46-50.
- Clarke, R. H. and G. D. Hess (1975): On the Relation Between Surface Wind and Pressure Gradient, Especially in Lower Latitudes, Boundary-Layer Meteor., 9(3), 325-339.
- Charnock, H. (1955): Wind Stress on a Water Surface, Quart. J. Roy. Meteor. Soc., 81(350), 639-640.
- Csanady, C. T. (1967): On the "Resistance Law" of a Turbulent Ekman Layer, J. Atmos. Sci., 24(5), 467-471.
- Deacon, E. L. (1973a): Geostrophic Drag Coefficients, Boundary-Layer Meteor., 5(3), 321-340.
- Deacon, E. L. (1973b): The Wind Profile under low U_* Conditions, Quart. J. Roy. Meteor. Soc., 99(420), 391-393.

- Garrett, J. R. (1973): Studies of Turbulence in the Surface Layer over Water (Lough Neagh). III. Wave and Drag Properties of the Sea-Surface in Conditions of Limited Fetch, Quart. J. Roy Meteor. Soc., 99(419), 35-47.
- Gill, A. E. (1968): Similarity Theory and Geostrophic Adjustment, Quart. J. Roy. Meteor. Soc., 94(402), 586-588.
- Grose, Peter L., James S. Mattson, Ed. (1977): The 'Argo Merchant' Oil Spill, NOAA Envir. Data Svc., Environmental Research Laboratories, 133 pp.
- Hasse, L. (1974): Note on the Surface-to Geostrophic Wind Relationship from Observations in the German Bight, Boundary-Layer Meteor., 6(1/2), 197-201.
- Hasse, L. (1974): On the Surface to Geostrophic Wind Relationship at Sea and the Stability Dependence of the Resistance Law, Beitrag Physik der Atmos., 47(1), 45-55.
- Hasse, L. and M. Dunckel (1974): Direct Determination of Geostrophic Drag Coefficients at Sea, Boundary-Layer Meteor., 7(3), 323-329.
- Hess, G. D. (1973): On Rossby-Number Similarity Theory for a Baroclinic Planetary Boundary Layer, J. Atmos. Sci., 30(8), 1722-1723.
- Hess, G. D. (1974): Determination of the Sea Surface Stress and Drift Current by Similarity Theory, Radiological and Environmental Research Division Annual Report, Argonne National Laboratory, ANL-75-3, Part IV, 112-119.
- Hicks, B. B. (1972): Some Evaluations of Drag and Bulk Transfer Coefficients over Water Bodies of Different Sizes, Boundary-Layer Meteor., 3(2), 201-213.
- Hicks, B. B. (1975): A Procedure for the Formulation of Bulk Transfer Coefficients over Water Bodies of Different Sizes, Boundary-Layer Meteor., 8(3/4), 515-524.
- Hoxit, L. R. (1975): Planetary Boundary Layer Winds in Baroclinic Conditions, J. Atmos. Sci., 31(4), 1003-1020.
- Hsu, S. A. (1974): On the Log-Linear Wind Profile and the Relationship Between Shear Stress and Stability Characteristics over the Sea, Boundary-Layer Meteor., 6(3/4), 509-514.
- Hsu, S. A. (1976): Determination of the Momentum Flux at the Air-Sea Interface under Variable Meteorological and Oceanographic Conditions: Further Application of the Wind-Wave Interaction Method, Boundary-Layer Meteor., 10(2), 221-226.

- Ichiye, T. (1972): Hydrodynamic Problems Concerning Oil Spillage in the Ocean, In Texas A & M University Sea Grant Report TAMU-SG-73-201, December 1972, 445 pp.
- Lange, Philipp & Heinrich Hühnerfuss (1978): Drift Response of Monomolecular Slicks to Wave and Wind Action, J. Phys. Oceanogr., 8(1), 142-150.
- Ruggles, K. W. (1970): The Vertical Mean Wind Profile Over the Ocean for Light to Moderate Winds, J. Applied Meteor., 9(3), 389-395.
- SethuRamen, S. and G. S. Raynor (1975): Surface Drag Coefficient Dependence on the Aerodynamic Roughness of the Sea, J. Geophys. Res., 80(36), 4983-4988.
- Smith, J. E., Ed. (1968): 'Torrey Canyon' Pollution and Marine Life, Cambridge U. Press, 196 pp.
- Smith, S. D. and E. G. Banke (1975): Variation of the Sea Surface Drag Coefficient with Wind Speed, Quart. J. Roy. Meteor. Soc., 101 (429), 665-673.
- Stolzenbach, Keith D., Ole S. Madsen, E. Eric Adams, Andrew M. Pollack, and Cortis K. Cooper (1977): A Review and Evaluation of Basic Techniques for Predicting the Behavior of Surface Oil Slicks, Ralph M. Parsons Laboratory for Water Resources and Hydrodynamics, Report 222, MIT, 44 pp.
- Swinbank, W. C. (1974): The Geostrophic Drag Coefficient, Boundary-Layer Meteor., 7(1), 125-127.
- Thompson, R. O. R. Y. (1974): The Influence of Geostrophic Shear on the Cross-Isobar Angle of the Surface Wind, Boundary-Layer Meteor., 6(3/4), 515-518.
- Wesly, James, Roy W. Hann, Jr., David Basco, Daniel M. Bragg, Joseph F. Osoba, Jack Dameron, Douglas von Gonten, Takashi Ichiye, and Rezneat Darnell (1972): Environmental Aspects of a Supertanker Port on the Texas Gulf Coast, Texas A and M University Sea Grant Report TAMU-SG-73-201, December 1972, 445 pp.
- Wieringa, J. (1974): Comparison of Three Methods for Determining Strong Wind Stress over Lake Flevo, Boundary-Layer Meteor., 7(1), 3-19.
- Wippermann, F. (1972): Baroclinic Effects on the Resistance Law for the Planetary Boundary Layer of the Atmosphere, Beitrage Physik der Atmos., 45(3), 244-259.
- Wippermann, F. (1972): A Note on the Parameterization of the Large-Scale Wind Stress at the Sea-Surface, Beitrage Physik der Atmos., 45(3), 260-266.

- Wippermann, F. (1974): The Parameterization of the Large-Scale Wind Stress at the Sea-Surface (Second Note), Beitrage Physik der Atmos., 47(4), 227-234.
- Wippermann, F. (1974): The Influence of Nonstationarity on the Surface-Stress Determined by the Resistance Law, Izvestiya, Atmos. and Oceanic Physics, 10(6), 646-647.
- Wu, J. (1969): Wind Stress and Surface Roughness at Air-Sea Interface, J. Geophys. Res., 74(2), 444-455.